Bulletin of the Seismological Society of America, 91, 6, pp. 1867–1874, December 2001

Attenuation of High-Frequency *P* and *S* Waves in the Crust of Southeastern South Korea

by Tae-Woong Chung and Haruo Sato

Abstract The seismicity of the Yangsan fault in southeastern S. Korea has received increasing attention recently because the fault lies in an industrial area. For this fault region, we first measured Q_P^{-1} and Q_S^{-1} simultaneously by applying the extended coda-normalization method to seismograms at nine stations of a network deployed by the Korea Institute of Geology, Mining, and Materials. We analyzed 707 seismograms of local earthquakes that occurred between December 1994 and February 2000. From velocity seismograms, bandpass-filtered traces were made by applying a phaseless four-pole butterworth filter with five octave-width frequency bands, 1–2, 2–4, 4–8, 8–16, and 16–32 Hz. Estimated Q_P^{-1} and Q_S^{-1} values decrease from $(7 \pm 2) \times 10^{-3}$ and $(5 \pm 4) \times 10^{-3}$ at 1.5 Hz to $(5 \pm 4) \times 10^{-4}$ and $(5 \pm 2) \times 10^{-4}$ at 24 Hz, respectively. By fitting power-law frequency dependence to the estimated values over the whole stations, we obtained $0.009\, f^{-1.05}$ for Q_P^{-1} and $0.004\, f^{-0.70}$ for Q_S^{-1}, where f is frequency in Hz. These results indicate that Q_P^{-1} and Q_S^{-1} in the crust of southeastern S. Korea are the lowermost of the reported values in the world, although the exponent values agree well with those in the other areas.

Introduction

The Q^{-1} value, amplitude attenuation with travel distance of seismic waves, is a very important parameter used to infer the material and physical conditions of the earth's interior. In particular, the knowledge of the Q^{-1} value is indispensable for the quantitative prediction of strong ground motion from the viewpoint of earthquake-resistant design of construction. Hence numerous studies of Q^{-1} have been undertaken worldwide and concentrated mainly on seismically active zones and/or densely populated industrial areas (e.g. Frankel *et al.*, 1990; Kinoshita, 1994). These studies show relatively higher Q^{-1} in seismically active areas than in stable areas (Sato and Fehler, 1998). There are several mechanisms of seismic-wave attenuation. One is scattering due to small-scale heterogeneities widely distributed in the lithosphere, and another is intrinsic absorption mostly controlled by thermal condition (Aki, 1980; Blakeslee *et al.*, 1989; Lees and Linley, 1994).

In S. Korea, the Yangsan fault (Fig. 1) has been receiving increasing attention because the fault lies in the industrial region where nuclear power plants are located. In Korean history, this fault is believed to have been responsible for a large earthquake that caused more than 100 deaths in A.D. 779 (Lee, 1998). On 26 June 1997, an earthquake with magnitude (M) 4.3 took place near the fault (star in Fig. 1), although S. Korea is far from a seismically active plate boundary, and earthquakes over M 4 have not frequently occurred in this century.

The Yangsan fault trending NNE–SSW is about 200 km long and runs parallel with other subsidiary faults such as Miryang, Moryang, Ulsan, and Tongre faults (solid and dashed lines in Fig. 1). These faults are developed mainly in the area of Cretaceous sediments that were intruded by igneous rocks in the Cretaceous to the Tertiary (Chang, 1987). Right-lateral displacements of these faults took place in the early Quaternary (Sillitoe, 1977; Otsuki and Ehiro, 1978), and a possibility for their recurrence is suggested (Lee *et al.*, 1984; Lee and Jin, 1991; Choi *et al.*, 1998). The focal mechanism analysis of several events in Korea suggests that the direction of the maximum compressional stress is ENE–SWS (e.g., Baag *et al.*, 1998).

In the Yangsan fault area, a regional seismic network has been in operation by the Korea Institute of Geology, Mining and Materials (KIGAM) since December 1994 (solid squares in Fig. 1). Based on the network data, Kim *et al.* (1999) first measured very low Q^{-1} for P waves (hereafter, Q_P^{-1}); however, the value was derived from only 10 earthquake data points. There have been no reports on Q^{-1} for S waves (hereafter, Q_S^{-1}) in S. Korea. In this article, using more than 120 earthquakes recorded by the network from 1994 to 2000, we first make the simultaneous measurement of Q_P^{-1} and Q_S^{-1} by means of the coda-normalization method.

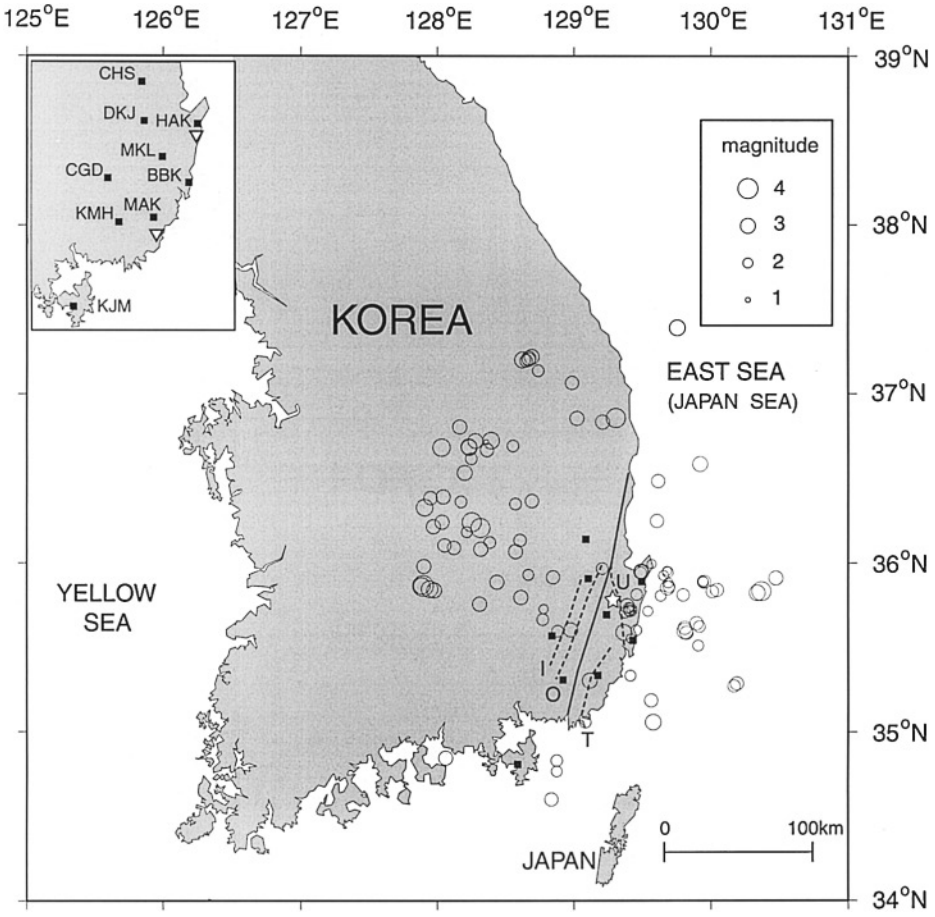

Figure 1. Map of Korea showing seismic stations (solid squares) and epicenters (open circles) of 121 earthquakes used in this study, as well as the Yangsan fault systems. Solid line represents the main fault, and dashed lines are subfaults: symbols I, O, U, and T show the Miryang fault, the Moryang fault, the Ulsan fault, and the Tongre fault, respectively. An asterisk represents the epicenter of the earthquake of 26 June 1997 (M 4.3). The inset in the upper left shows atomic power plants (reverse triangles) and the seismic stations of KIGAM with the abbreviation names.

Method of Analysis

In this study, Q_P^{-1} and Q_S^{-1} in the crust of the southeastern Korea are estimated by using the extended coda-normalization method (Yoshimoto *et al.*, 1993), which is an extension of the conventional coda normalization method (Aki, 1980). It is based on the following proportionality among the coda spectral amplitude C, the source spectral amplitude of S waves S_S, and the source spectral amplitude of P waves S_P,

$$C(f,t_C) \propto S_S(f) \propto S_P(f), \tag{1}$$

where f is frequency in Hz and t_C is a fixed lapse time in sec measured from the source origin time. The lapse time was chosen to be greater than 1.5 to 2 times the S-wave travel time. The first proportionality implies that $C(f,t_C)$ is independent of the hypocentral distance: site and source terms that are common in direct waves and coda can be removed by the coda normalization (Aki, 1980). The second proportionality is deduced from the assumption that the ratio of P- to S-wave source spectra is constant for a small range of magnitudes. Differences in radiation pattern are expected to be smoothed if the number of earthquakes is sufficiently large.

Based on the aforementioned proportionality, a ratio of a product of hypocentral distance and direct amplitude to coda amplitude exponentially decreases with hypocentral distance. The logarithm of the ratio linearly decreases with hypocentral distance,

$$\ln\left[\frac{A_P(f,r)r}{C(f,t_C)}\right] = -\frac{\pi f}{Q_P(f)V_P}r + const(f), \tag{2}$$

$$\ln\left[\frac{A_S(f,r)r}{C(f,t_C)}\right] = -\frac{\pi f}{Q_S(f)V_S}r + const(f), \tag{3}$$

where $A_P(f,r)$ and $A_S(f,r)$ are the direct P- and S-wave maximum amplitudes at the hypocentral distance r (km), respec-

tively. Applying the least-squares method to plots of the left-hand side (LHS) of (2) and (3) against the hypocentral distance for many earthquakes, we can estimate Q_P^{-1} and Q_S^{-1} from linear regression lines. The *P*-wave analysis was based on U–D component seismograms, and the *S*-wave analysis was based on the N–S component, since significant amplitude differences were not observed between the N–S and E–W components.

The coda spectral amplitude was derived from the root-mean-square (rms) amplitude for the time window of 5 sec centered at $t_C = 60$ sec. Coda waves of lapse time up to 60 sec sample a volume having a radius of about 100 km, roughly speaking. The span of 5 sec was also chosen for both the *P*- and *S*-wave time window to pick the maximum amplitude of direct arrivals (Fig. 2a). Some seismograms show a phase reflected from Moho (*Sm*S) just after the *Sg* phase. The later phase was excluded by narrowing the *S*-wave window (see Fig. 2b). In some record sections at hypocentral distances greater than about 120 km, it is hard to discriminate *Sg* from *Sm*S and *Lg* because they are too close each other. We excluded these kinds data from our data set. Such a distinct difference of phase amplitudes was not observed in *P*-wave data.

We subtracted the noise power spectra sampled with a lapse of 5 sec prior to the *P*-wave arrival from the spectral amplitudes of *P*- and *S*-wave arrivals and coda spectra, assuming that the signal and noise are statistically independent and that the noise is stationary. We found that the noise subtraction reduced the coda spectral amplitude for events of small magnitudes and hence improved linearity between magnitude and the coda spectral amplitude. Since the linearity was suggested by the coda observations (Tsumura 1967a,b; Tsujiura, 1978), the subtraction of noise power spectra was plausible in this study. Then, we discarded data with signal power spectra of less than twice the noise power spectra.

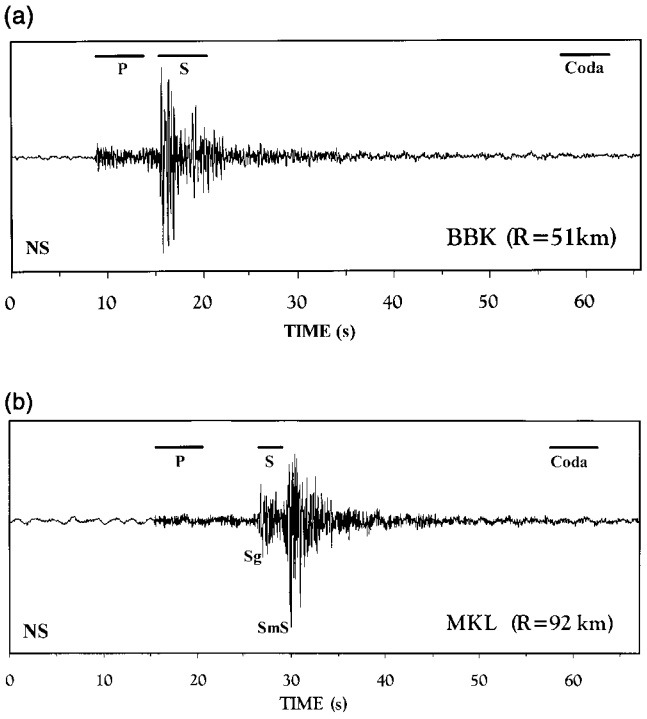

Figure 2. Typical example of time windows of direct *P* and S waves and coda for a raw seismogram recorded at station BBK. (b). An example of seismogram at station MKL, where the time window of a direct *S* waves (*Sg*) is narrower than that in Figure 2a to exclude the high amplitude phase of *Sm*S.

Data

A seismic network operated by KIGAM around the Yangsan fault consists of nine stations: Duk-jung (DKJ), Myung-kye-li (MKL), Chung-song (CHS), Bang-bang-kol (BBK), Hak-gye (HAK), Kim-hae (KMH), Ku-je-myon (KJM), Mae-gok (MAK), and Chung-do (CGD). A three-component velocity seismograph is installed at every station, where its natural frequency is 0.05 Hz at CHS and KJM and 1 Hz at other stations (Chi *et al.*, 1996). Observed seismograms are digitized with a sampling interval of 0.02 or 0.01 sec.

We analyzed 707 seismograms of local earthquakes that occurred from December 1994 to February 2000. Hypocenters and local magnitudes of 392 seismograms of 109 events were routinely determined by KIGAM based on the model with *P*-wave velocities of 5.98 km/sec (0–15 km in depth), 6.38 km/sec (15–35 km in depth), and 7.95 km/sec (35 km in depth) (Kim and Kim, 1983). For 45 seismograms, we located 12 events using the code HYPO71 (Lee and Lahr, 1972) for the same model used by KIGAM. The remaining 270 seismograms of relatively far events are recorded at a single station or two stations. Hypocentral distances of these earthquakes were estimated from their *S*-*P* times. The local magnitudes of all the events range from 1.8 to 3.9.

To take the same window span of *P*-wave signal with that of coda, we selected seismograms with *S*-*P* times larger than 5 sec, which correspond to the hypocentral distance longer than about 40 km. Hypocentral distances, in addition, were limited within 160 km because the relation between coda duration and magnitude changes with increasing hypocentral distances, especially for longer than 200 km (Tsumura, 1967b).

Measurements of Q_P^{-1} and Q_S^{-1}

We removed a trend and mean value from each velocity seismogram and applied a cosine taper to both ends of data for a width of 10% of the full time length. Then, seismograms were filtered by using a phaseless four-pole butterworth filter with five octave-width frequency bands, 1–2, 2–4, 4–8, 8–16, and 16–32 Hz. The maximum *P*- and *S*-wave arrivals, $A_P(f, r)$ and $A_S(f, r)$ in equations (2) and (3), were measured from U–D and N–S components of seismograms, respectively. The coda spectral amplitude was derived from

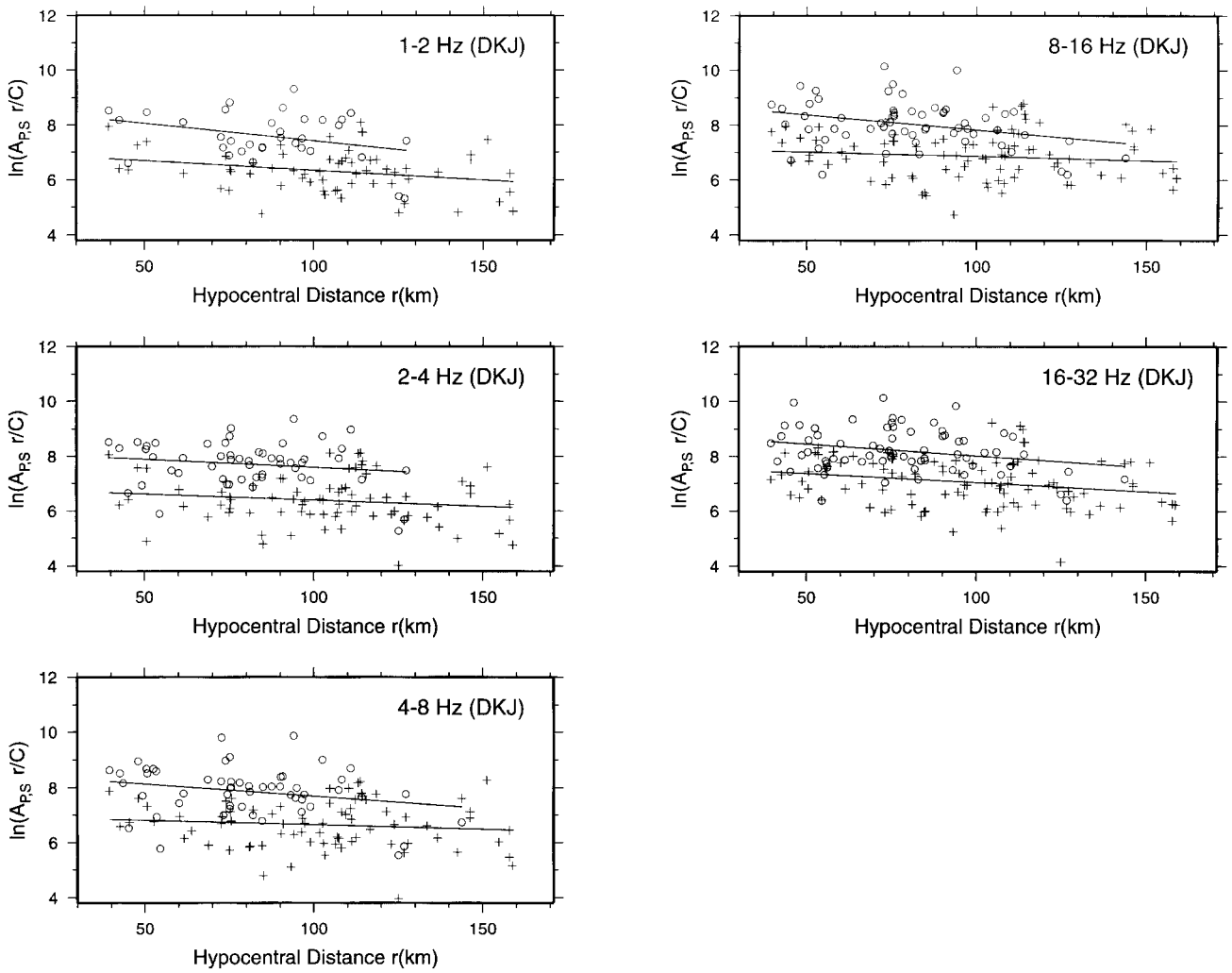

Figure 3. Plots of the left-hand side of equations (2) and (3) against hypocentral distance for *P* (crosses) and *S* (circles) waves, respectively, recorded at station DKJ. The regression lines from the least-squares estimate are expressed by two solid lines: the upper and lower lines are for *S*- and *P*-wave amplitude, respectively.

the same component of the arrivals targeted for the coda normalization. In Figure 3, we plot the LHS of equations (2) and (3) against hypocentral distance for five frequency bands at station DKJ as an example. Finally, Q_P^{-1} and Q_S^{-1} were obtained from the gradients of the linear regression lines at each station, where we put $V_P = 6.0$ km/sec and $V_S = 3.5$ km/sec. We plot the arithmetic mean of Q_P^{-1} and Q_S^{-1} and their standard deviations in five frequency bands at nine stations in Figure 4.

The number of *P*-wave data in DKJ was 61, 80, 81, 92, and 110 in the frequency range of 1–2, 2–4, 4–8, 8–16, and 16–32 Hz, respectively. For the corresponding frequency range, the number of the S-wave data was 37, 61, 60, 66, and 80, respectively. We enumerate the number of data used for the estimation of Q_P^{-1} and Q_S^{-1} at each station in Table 1. The number of data increased with a gain of central frequencies. The small number in the 1- to 2-Hz range was due to large noise probably induced by sea waves. The high-frequency data showed smaller scatter around the regression line compared to the low-frequency data. In some frequency band at some station such as KMH, MAK, KJM, and CGD showed the regression line with a positive gradient leading to negative Q_P^{-1} and/or Q_S^{-1} caused by insufficient number of data. Q_P^{-1} and Q_S^{-1} values at CGD is less reliable since the number of data used is small. However, the positive slopes were also observed for the *P*-wave regression line in MKL, the second largest number of data in the stations. This was due to the high amplitude data between the hypocentral distance of 110 and 150 km that originated from earthquakes that occurred at a NW directional region. These negative Q^{-1} values are excluded in the plots shown in Figure 4. We note that there is no possibility that site effects lead to negative Q^{-1} because these stations are located on hard-rock sites.

We found strong frequency dependence from the plots of Q_P^{-1} and Q_S^{-1} for each station in Figure 4. Q_P^{-1} and Q_S^{-1}

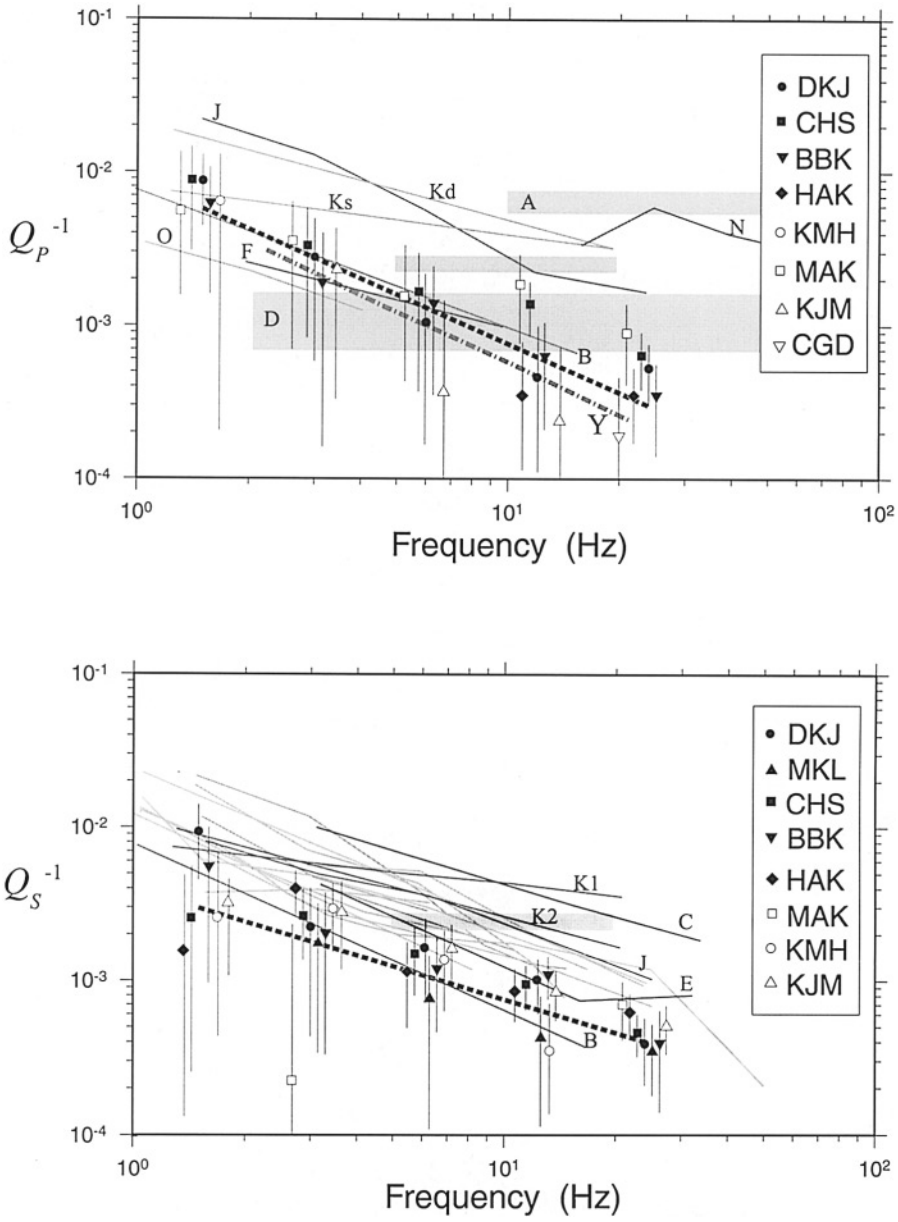

Figure 4. Q_P^{-1} (upper) and Q_S^{-1} (lower) measured in the southeastern Korea, where the error bars indicate the standard deviation. Bold broken lines refer to the best-fit regression lines by the least squares. A gray-chained line denoted by Y refers to the study on the same area based on the reversed two-station method (Kim *et al.*, 1999). A gray area designated by A and D, and thick lines by O, J, F, N, B, C, and E refer to the following studies; A, Arette, France (Modiano and Hatzfeld, 1982); D, drill hole in southern California (Abercrombie, 1995); O, shield region in North America (Taylor *et al.*, 1986); J, Kanto in Japan (Yoshimoto *et al.*, 1993), F, France (Campillo and Plantet, 1991); N, Nagano in Japan (Yoshimoto *et al.*, 1998); B, Baltic shield (Kvamme and Havskov, 1989); C, southern California; and E, New York State (Frankel *et al.*, 1990), respectively. The lines denoted by Ks, Kd, K1, and K2 refer to measurements in southern Kurils for the focal depth ranges of 5–55 km, 55–85 km, 5–25 km, and 25–55 km, respectively (Fedotov and Boldyrev, 1969). Gray areas or lines show the reported measurements in the world (modified from Sato and Fehler, 1998).

Table 1
The Number of Data Used for the Estimation of Q_P^{-1} and Q_S^{-1} at Each Station

Station	1–2 Hz		2–4 Hz		4–8 Hz		8–16 Hz		16–32 Hz	
	a = Q_P^{-1}	b = Q_S^{-1}	a = Q_P^{-1}	b = Q_S^{-1}	a = Q_P^{-1}	b = Q_S^{-1}	a = Q_P^{-1}	b = Q_S^{-1}	a = Q_P^{-1}	b = Q_S^{-1}
DKJ	61	37	80	61	81	60	92	66	110	80
MKL	59	38	65	45	67	47	67	49	83	55
CHS	42	39	61	53	63	55	63	59	64	59
BBK	33	26	45	34	55	33	61	34	59	39
HAK	25	21	47	25	57	29	55	33	58	39
KMH	28	19	33	25	33	25	36	28	37	29
KJM	21	12	27	16	27	16	27	16	27	16
MAK	20	16	25	22	23	18	21	18	22	20
CGD	14	5	13	5	13	5	13	7	14	7

decreased from $(7 \pm 2) \times 10^{-3}$ and $(5 \pm 4) \times 10^{-3}$ and at 1.5 Hz to $(5 \pm 4) \times 10^{-4}$ and $(5 \pm 2) \times 10^{-4}$ at 24 Hz, respectively. The standard deviations represented by error bars are smaller in higher frequencies than those in lower frequencies. Fitting a power law dependence on frequency, we found that the best fit Q_P^{-1} and Q_S^{-1} are $0.009\ (\pm 0.003) f^{-1.05(\pm 0.14)}$ and $0.004\ (\pm 0.001) f^{-0.70(\pm 0.14)}$, respectively. In the least-squares method, the reciprocal of the standard deviation is used as the weight at each station, and events having negative Q^{-1} are excluded. These best-fit power-law lines are shown by bold broken lines in Figure 4.

The stations names listed in Figure 4 are arranged in descending order of the number of data used for the station. Solid symbols, denoting a relatively sufficient number of data, showed smaller scatter around the best-fit lines in Q_P^{-1} and Q_S^{-1}. The best-fit line for Q_P^{-1} shows a good agreement with the measurement (gray chained line) by Kim *et al.* (1999), which was carried out in the same area based on the reversed two-station method using a two-station spectral ratio for aligned two sources (Chun *et al.*, 1987).

Discussion

For comparison, measurements of Q_P^{-1} and Q_S^{-1} at several areas in the world are also shown by shaded lines or areas in Figure 4. These plots include attenuation not only in the crust but also in the uppermost mantle. For the values derived from the events within the hypocentral range of 300 km, seismically stable regions such as the Baltic shield (Kvamme and Havskov, 1989) have low Q_P^{-1} values, while seismically active regions such as Kanto in Japan (Yoshimoto *et al.*, 1993) and southern Kurils (Fedotov and Boldyrev, 1969) show high Q_P^{-1} values. In southern Kuril, the Q_P^{-1} value obtained from the events with a focal depth of 55–85 km is higher than that from the events with 5–55 km. However, shallow parts of the earth generally show higher Q^{-1} than deeper parts of the earth. From the measurements with hypocentral distances less than 40 km, a high Q_P^{-1} value is observed for Arette in France (Modiano and Hatzfeld, 1969) and Nagano in Japan (Yoshimoto *et al.*, 1998). On the other hand, the *Pg* study of events for the epicentral distance between 200 and 1000 km shows very low Q_P^{-1} values in France (Campillo and Plantet, 1991). The teleseismic study over epicentral distances of 50° show that the Q_P^{-1} value of the Basin and Range in North America (Taylor *et al.*, 1986) is indistinguishable from that of Baltic shield. This teleseismic study indicates that Q_P^{-1} for shield regions in North America is lower value than those described previously. Correspondingly low Q_P^{-1} value is observed from the down hole measurement at a depth of 2.5 km even in seismically active region, southern California (Abercrombie, 1995). Our best-fit line (bold broken line) and the previous study by Kim *et al.* (1999) (gray chained line) lie in the lowest portion of surface measurements.

Since there were numerous studies of Q_S^{-1} compared to Q_P^{-1}, we focus on Q_S^{-1} measurements on the ground surface for the similar depth range with the hypocentral distances between 90 and 300 km. A remarkable difference of Q_S^{-1} is observed between New York State and southern California, which are seismically inactive and active regions, respectively (Frankel *et al.*, 1990). Such a difference is also observed for the other regions as the same for Q_P^{-1}: Baltic shield for a stable region and southern Kurils and Kanto in Japan for active regions. Our best-fit line of Q_S^{-1} (bold broken line) corresponds to those for Baltic shield, which lies in the lowest portion of the Q_S^{-1} values reported. However, the frequency dependence of the best-fit line, indicated by the gradient, is very similar to that of the past measurements for both Q_P^{-1} and Q_S^{-1} in other areas. Coda Q^{-1} measured based on the same network data (Jun *et al.*, 1995; Baag, 1997; Lee and Lee, 1998) also shows similar values with those of central and eastern North America, which are seismically stable regions (Toro *et al.*, 1997).

The precise velocity structure of S. Korea has not been known yet. One layer model was first obtained with a 5.8 km/sec *P*-wave velocity of 35-km thickness for the crust (Lee, 1979). Although the two-layer model for the crust (Kim and Kim, 1983) is now widely used for the hypocentral location, there is still controversy over whether the one- or two-layer model is better (e.g., Lee and Chung, 1999). The velocity model affects not only the shape of scattering shell in the coda envelope synthesis but also the direct-wave am-

plitude (e.g., Sato and Fehler, 1998). The estimation of Q^{-1} values, however, depends mainly on the choice of background velocities as given in equations (2) and (3) and is not so sensitive to the choice of velocity model. In the future, we need to introduce the depth dependence of both velocity and scattering coefficients in the attenuation measurements as Yoshimoto (2000) recently synthesized coda envelopes.

In this study, we did not observe high Q^{-1} values associated with fracturing and crack accumulation (e.g., Lees and Lindley, 1994) due to the activity of the Yangsan fault. The Q^{-1} value estimated in this region is as low as that of shield, which is a seismically stable region. The Q^{-1} value might be related to the heat flows because the mechanism studies show that Q^{-1} increases with increasing temperature (e.g., Jackson and Anderson, 1970). The low heat flows have been observed in shields with about 40 mW/m^2, while the global average of continents is 65 mW/m^2 (Pollack and Chapman, 1977; Pollack *et al.*, 1993). On the other hand, high values more than 80 mW/m^2 were suggested around the Yangsan fault, which seems to be related to high heat flows at the Sea of Japan (Han and Chapman, 1985). Even though seismicity is high, the value of less than 40 mW/m^2 is observed for Kanto, Japan. The inconsistency between the heat flow and seismicity has been observed for many regions (e.g., Sclater *et al.*, 1980). Physical interpretation based on more detailed measurements is required in studying seismic wave attenuation in southeastern S. Korea.

Conclusion

The seismicity of the Yangsan fault in southeastern S. Korea is important because the fault lies in an industrial area. The knowledge of seismic-wave attenuation is very necessary for the quantitative prediction of strong ground motion. We first simultaneously estimated Q_P^{-1} and Q_S^{-1} by applying the extended coda-normalization method to seismic network data in this area. Estimated Q_P^{-1} and Q_S^{-1} decrease from $(7 \pm 2) \times 10^{-3}$ and $(5 \pm 4) \times 10^{-3}$ and at 1.5 Hz to $(5 \pm 4) \times 10^{-4}$ and $(5 \pm 2) \times 10^{-4}$ at 24 Hz, respectively. By fitting power-law frequency dependence to data over the whole stations, we obtained $0.009\ (\pm 0.003) f^{-1.05(\pm 0.14)}$ for Q_P^{-1} and $0.004\ (\pm 0.001) f^{-0.70(\pm 0.14)}$ for Q_S^{-1}. These results indicate that Q_P^{-1} and Q_S^{-1} values in southeastern S. Korea are some of the lowest in the world, although the exponent values agree well with those in the other areas. The low Q_P^{-1} and Q_S^{-1} values correspond to those of the seismically stable regions such as shields.

Acknowledgments

The authors are grateful for help and advice from Kazuo Yoshimoto. We thank reviewers R. R. Castro and K. Lee, whose comments were very helpful for revising the manuscript. This article was accomplished with the Research Fund provided by the Korea Research Foundation, Support for Faculty Research Abroad, during the stay of the first author (T.W.C.) at the Tohoku University in Sendai.

References

Abercrombie, R. E. (1995). Earthquake source scaling relationship from −1 to 5 M_L using seismograms recorded at 2.5-km depth, *J. Geophys. Res.* **100,** 24,015–24,036.

Aki, K. (1980). Attenuation of shear waves in the lithosphere for frequencies from 0.05 to 25 Hz, *Phys. Earth Planet. Interiors* **21,** 50–60.

Baag, C. E. (1997). Seismic wave attenuation in the Korea Peninsula, Research Report of Korea Atomic Energy Research Institute KAERI-96-08, 1–43 (in Korean).

Baag, C. E., J. S. Shin, H. C. Chi, I. B. Kang, Y. Ryoo (1998). Fault-plane solutions of the December 13, 1996 Yeongweol earthquake, *J. Korean Geophys. Soc.* **1,** 23–30.

Blakeslee, S., P. Malin, and M. Alvarez (1989). Fault-zone attenuation of high-frequency seismic waves, *Geophys. Res. Lett.* **16,** 1321–1324.

Campillo, M., and J. L. Plantet (1991). Frequency dependence and spatial distribution of seismic attenuation in France: experimental results and possible interpretations, *Phys. Earth Planet. Interiors* **67,** 48–64.

Chang, K. H. (1987). Cretaceous strata, in *Geology of Korea*, D. S. Lee (Editor), Kyohak-Sa Pub. Co., Seoul, 175–193.

Chi, H. C., J. S. Jun, and I. C. Shin (1996). Seismological study at the Kyungsang Basin (III), *KIGAM Research Report*, KR-96(C)-4, 127 pp. (in Korean).

Choi, U., D. Y. Lee, B. J. Lee, C. R. Ryoo, P. Y. Choi, S. J. Choi, D. L. Cho, J. Y. Kim, C. B. Lee, W. S. Kee, D. Y. Yang, I. J. Kim, Y. Kim, J. H. Yoo, B. G. Chae, W. Y. Kim, P. J. Kang, I. H. Yu, and H. K. Lee, (1998). An investigation and evaluation of capable fault: southeastern part of the Korean Peninsula, KIGAM Research Report, KR-98(C)-22, 301 pp. (in Korean).

Chun, K. Y., G. F. West, R. J. Kokoski, and C. Samson (1987). A novel technique for measuring Lg attenuation: results from Eastern Canada between 1 to 10 Hz, *Bull. Seism. Soc. Am.* **77,** 398–419.

Fedotov, S. A., and S. A. Boldyrev (1969). Frequency dependence of the body-wave absorption in the crust and the upper mantle of the Kuril Island chain, *Izv. Acad. Sci. USSR* **9,** 17–33.

Frankel, A., A. McGarr, J. Bicknell, J. Mori, L. Seeber, and E. Cranswick (1990). Attenuation of high-frequency shear waves in the crust: measurements from New York State, South Africa and Southern California, *J. Geophys. Res.* **95,** 17,441–17,457.

Han, W., and D. S. Chapman (1985). On the regional heat flow around Korea and reduced heat flow, *J. Geol. Soc. Korea* **21,** 79–89.

Jackson, D. D., and D. L. Anderson (1970). Physical mechanism of seismic wave attenuation, *Rev. Geophys. Space Phys.* **8,** 1–63.

Jun, M. S., H. C. Chi, J. S. Jun, and I. C. Shin (1995). Seismological study around Yangsan fault in 94, KIGAM Research Report, KR-94(C), 1–16 (in Korean).

Kim, S. J., and S. G. Kim (1983). A study on the crustal structure of south Korea by using seismic waves, *J. Korean Inst. Mining Geol.* **16,** 51–61 (in Korean).

Kim, S. K., M. S. Jun and J. K. Kim (1999). Attenuation of P-waves in the Kyungsang Basin, Southeastern Korea, *J. Geol. Soc. Korea* **35,** 223–228 (in Korean).

Kinoshita, S. (1994). Frequency-dependent attenuation of shear waves in the crust of the southern Kanto area, Japan, *Bull. Seism. Soc. Am.* **84,** 1387–1396.

Korea Institute of Geology, Mining, and Materials. Open Web Data, *http://quake.kigam.re.kr/html/frame4.htm*, (last accessed October 2001).

Kvamme, L. B., and J. Havskov (1989). Q in southern Norway, *Bull. Seism. Soc. Am.* **79,** 1575–1588.

Lee, K. (1979). On crustal structure of the Korean Peninsula, *J. Geol. Soc. Korea* **15,** 253–258.

Lee, K. (1998). Historical earthquake data of Korea, *J. Korean Geophys. Soc.* **1,** 3–22 (in Korean).

Lee, K., B. I. Jeong, Y. H. Kim, and S. J. Yang (1984). A geophysical study of the Yangsan fault area, *J. Geol. Soc. Korea* **20,** 222–240.

Lee, K., and T. W. Chung (1999). A comparative study on the crustal structure models using microearthquakes in the southeastern part of the Korean peninsula from 1995 to 1996, *J. Korean Geophys. Soc.* **2,** 1–8.

Lee, K., and Y. G. Jin (1991). Segmentation of the Yangsan fault system: geophysical studies on major faults in the Kyeongsang basin, *J. Geol. Soc. Korea* **27,** 434–449.

Lee, W. H. K., and J. C. Lahr (1972). HYPO71: A computer program for determining hypocenter, magnitude, and first motion pattern of local earthquakes, *U.S. Geol. Surv. Open-File Rept. 75–311.*

Lee, W. S., and K. Lee (1998). Q estimates using the coda waves in the Kyungsang Basin, Proceedings of EESK Conference, 1998.

Lees, J. M., and G. T. Lindley (1994). Three-dimensional attenuation tomography at Loma Prieta: Inversion of t* for Q, *J. Geophys. Res.* **99,** 6843–6863.

Modiano, T., and D. Hatzfeld (1982). Experimental study of the spectral content for shallow earthquakes, *Bull. Seism. Soc. Am.* **72,** 1739–1758.

Otsuki, K., and M. Ehiro (1978). Major strike-slip faults and their bearing on spreading in the Japan Sea, *J. Phys. Earth*, **26** (suppl.), 537–555.

Pollack, H. N., and D. S. Chapman (1977). On the regional variation of heat flow, geotherms, and lithospheric thickness, *Tectonophysics* **38,** 279–296.

Pollack, H. N., S. J. Hurter, and J. R. Johnson (1993). Heat flow from the earth's interior: Analysis of the global data set, *Rev. Geophys. Space Phys.* **31,** 267–280.

Sato, H., and M. C. Fehler (1998). Seismic wave propagation and scattering in the heterogeneous earth, Springer-Verlag, New York, 308 pp.

Sclater, J. G., C. Jaupart, and D. Galson (1980). The heat flow through oceanic and continental crust and the heat loss of the Earth, *Rev. Geophys.* **18,** 269–311.

Sillitoe, R. H. (1977). Metallogeny of an Andean type continental margin in South Korea, implications for opening of the Japan Sea, in *Island Arcs*, *Deep Sea Trenches and Back Arc Basins*, Maurice Ewing Series M. Talwani and W. C. Pitman III (Editors), American Geophysical Union, Washington, D. C., Vol. 1, 303–310.

Taylor, S. R., B. P. Bonner, and G. Zandt (1986). Attenuation and scattering of broadband P and S waves across North America, *J. Geophys. Res.* **91,** 7309–7325.

Toro, G. R., N. A. Abrahamson, and J. F. Schneider (1997). Model of strong ground motions from earthquakes in central and eastern North America: best estimates and uncertainties, *Seism. Res. Lett.* **68,** 41–57.

Tsujiura, M. (1978). Spectral analysis of the coda waves from local earthquakes, *Bull. Earthquake Res. Inst. Univ. Tokyo* **53,** 1–48.

Tsumura, K. (1967a). Determination of earthquake magnitude from duration of oscillation, *Zisin* **20,** 30–40 (in Japanese).

Tsumura, K. (1967b). Determination of earthquake magnitude from total duration of oscillation, *Bull. Earthquake Res. Inst. Univ. Tokyo* **45,** 7–18.

Yoshimoto, K. (2000). Monte-Carlo simulation of seismogram envelope in scattering media, *J. Geophys. Res.* **105,** 6153–6161.

Yoshimoto, K., H. Sato, and M. Ohtake (1993). Frequency-dependent attenuation of P and S waves in the Kanto area, Japan, based on the coda-normalization method, *Geophys. J. Int.* **114,** 165–174.

Yoshimoto, K., H. Sato, Y. Ito, H. Ito, T. Ohminato, and M. Ohtake (1998). Frequency-dependent attenuation of high-frequency P and S waves in the upper crust in western Nagano, Japan, *Pure Appl. Geophys.* **153,** 489–502.

Department of Earth Sciences
Sejong University
Seoul 143-747, S. Korea
chungtw@sejong.ac.kr
(T.-W.C.)

Department of Geophysics
Graduate School of Science
Tohoku University
Sendai 980-8578, Japan
sato@zisin.geophys.tohoku.ac.jp
(H.S.)

Manuscript received 15 November 2000.